Natural Resources Canada | Ressources naturelles Canada

GEOLOGICAL SURVEY OF CANADA
OPEN FILE 9281

Standardized procedure for silt (63-10, 10-6, 6-2 µm) and clay (2-0.6, 0.6-0.2, < 0.2 µm) separations for mineral characterization and geochronology

L. Nania, J.W. Powell, A. Grenier, I. Bilot, and J.B. Percival

2025

Canada

GEOLOGICAL SURVEY OF CANADA
OPEN FILE 9281

Standardized procedure for silt (63-10, 10-6, 6-2 µm) and clay (2-0.6, 0.6-0.2, < 0.2 µm) separations for mineral characterization and geochronology

L. Nania, J.W. Powell, A. Grenier, I. Bilot, and J.B. Percival

2025

Recommended citation
Nania, L., Powell, J.W., Grenier, A., Bilot, I., and Percival, J.B., 2025. Standardized procedure for silt (63-10, 10-6, 6-2 µm) and clay (2-0.6, 0.6-0.2, < 0.2 µm) separations for mineral characterization and geochronology; Geological Survey of Canada, Open File 9281, 30 p. https://doi.org/10.4095/p4uapabesk

Publications in this series have not been edited; they are released as submitted by the author.

ISSN 2816-7155
ISBN 978-0-660-77533-3
Catalogue No. M183-2/9281E-PDF
https://doi.org/10.4095/p4uapabesk

ABSTRACT: When dealing with clay-rich samples, separating and identifying authigenic from detrital minerals into distinct subsamples are crucial steps in elucidating geological parameters for tectonic, economic and geochronological studies. The following report outlines a clay separation procedure employed at the Geological Survey of Canada to isolate authigenic and detrital minerals into different silt and clay fractions, quantifying non-clay minerals in the separated samples, and estimating the crystallinity index of clay minerals. The grain size of the fractions obtained using this procedure are examined using a laser particle size analyzer, while the identification of their mineralogical composition is achieved using X-ray diffraction analysis. This protocol provides guidelines for clay sample preparation before chemical and geochronological analyses to determine geological processes such as: diagenesis, weathering, faulting (fault slip and fluid circulation), and host-rock alteration associated with mineralization.

RÉSUMÉ: En présence d'échantillons riches en argile, séparer et identifier les minéraux authigènes des minéraux détritiques en sous-échantillons distincts est crucial pour les études géologiques. Ce rapport décrit la procédure utilisée à la Commission Géologique du Canada pour isoler ces minéraux en fractions de limon et d'argile, quantifier les minéraux non argileux et estimer l'indice de cristallinité des minéraux argileux. La taille des grains est examinée avec un granulomètre laser, et leur composition minéralogique est identifiée par diffraction des rayons X. Ce protocole fournit des lignes directrices pour la préparation des échantillons d'argile avant les analyses chimiques et géochronologiques pour étudier des processus géologiques comme la diagenèse, l'altération, les failles (glissement et circulation des fluides), et l'altération de la roche-hôte liée à la minéralisation.

1. INTRODUCTION

Clay minerals such as mica, chlorite, kaolinite, and mixed-layered clay minerals are typically produced by mineralogical transformations from diagenetic to mid-to-low temperature conditions in fluid-rich environments (Velde, 1985, with references therein). Specifically, their polytype, crystallinity and chemistry reflect the temperature at which they formed, from the diagenetic zone to the anchizone and epizone (Velde, 1985; Pevear, 1999; van der Pluijm et al., 2001). In modern sedimentary settings (e.g., glacial deposits), clay minerals are also used to infer the physical transport processes by comparing their abundance in various grain-size fractions with the possible sources of the original protolith (*cf*., Chamley, 1989; Aden et al., 2015). In fault zone and hydrothermally- altered basement rocks, nanoparticles of illite (0.02 μm) start nucleating from a supersaturated solution at diagenetic temperatures (Eberl et al., 1998), with well-formed crystalline grains at the micrometre scale, so that their age can be linked to specific geological events. Hence, comprehensive isotopic, geochemical, mineralogical, and geochronological analyses are used to constrain the timing of slip motion along faults, assessing post-faulting resetting/multiple re-activations, and for unraveling fluid circulation controlling the distribution of active and fossil hydrothermal systems, ore deposits and hydrocarbon reservoirs, relevant to our society (Garven et al., 1999; Zwingmann and Mancktelow, 2004; Cloutier et al., 2009; Richard et al., 2016; Ootes et al., 2018). Exploring the significance of a specific clay mineral, however, may not be straightforward. In fault zones, clay minerals can occur as authigenic (syn-kinematic) grains and detrital (older) grains (Pevear, 1999). Authigenic, syntectonic micas result from the fault's frictional heating and strain-induced mineral precipitation and can grow through processes such as continuous crystallization over prolonged shearing and/or multiple (fluid-enhanced) faulting events (Eberl et al., 1998; Torgersen et al., 2015a, b; Tartaglia et al., 2020). Detrital grains derive from mechanical mixing of older minerals from the host rock (Pevear, 1999). Similarly, in hydrothermal systems, multiple fluid events can introduce various mineralogical contributions, among which only one may be associated with a specific ore deposit or event of interest (Fulignati, 2020).

A fundamental step toward understanding the origin of clay minerals within a sample arise from chemical and mineralogical analyses revealing that detrital mica and authigenic illite typically exhibit distinct crystalline structures and levels of crystallinity (Pevear, 1999; van der Pluijm et al., 2001; Warr and Cox, 2016). X-ray diffraction (XRD) analysis can identify mineral

phases (including polytypes) in the clay-size separates, can determine their semi-quantitative abundance in these fractions, and elucidate illite and chlorite (i.e., clinochlore, sudoite, chlorite-smectite mixed-layered clay minerals, etc.) crystallinity using Kübler (1967) and Árkai (1991) standardizations (full-width-at-half-maximum, FWHM, of the *(001*) illite and *(002)* chlorite reflections, respectively). For instance, detrital micas are typically characterized by the higher temperature $2M_1$ polytype (igneous or metamorphic in origin), whereas authigenic illite occurs as the lower temperature $1M_d$ polytype, developed between diagenetic and low-grade metamorphic conditions (Velde, 1985; Pevear, 1999; van der Pluijm et al., 2001).

Through the comparison of ^{40}K-^{40}Ar ages with grain size, Torgersen and Viola (2014) and Torgersen et al. (2015a) also suggested an Age Attractor Model. This model asserts that, in clay-rich samples and fault zones, a positive relationship between ages and grain size exists, with the finest fractions representing the final increment of crystallization and, therefore, the authigenic grains (Hower et al., 1963; Torgersen et al., 2015a, b and references therein). Thus, only by combining mineralogical information for different grain size fractions and samples from an area of interest can we infer all the information listed above, to *i*) identify protolith-related minerals versus recrystallized grains; *ii*) estimate hydrothermal alteration paragenesis, to infer pH and temperature conditions of a geothermal system or hydrothermal ore deposits (Fulignati, 2020; McIntosh et al., 2021); *iii*) determine whether a clay-rich sample is datable using the ^{40}K-^{40}Ar geochronology (i.e., if the starting material has sufficient white mica/illite compared to non-datable minerals and which minerals can contribute to the bulk age); and *iv*) determine the temperature conditions of the alteration/faulting event.

Nonetheless, one of the most delicate aspects in separating clays into different size fractions (representative of the authigenic and detrital phases), is how to disaggregate the sample without artificially decreasing grain size of detrital minerals, which can occur during mechanical crushing (Kisch, 1991). Freezing and thawing methods for gentle disaggregation (Torgersen et al., 2015a, b) and centrifugation are commonly used to obtain particle sizes down to <0.2 µm (e.g., see Zwingmann et al., 2010; Torgersen et al., 2015a, b; Viola et al., 2016, 2018; Fulignati, 2020; Zheng et al., 2023). The Sedimentology Laboratory and the X-ray Mineralogy Laboratory at the Geological Survey of Canada (GSC) are equipped for clay-rich sample preparation and X-ray characterization of authigenic and detrital clay minerals. This report outlines recent progress on the sample disaggregation procedures employed at the Geological Survey of Canada, along with

X-ray diffraction-based methods used to identify and quantify mixtures of clays and non-clay minerals. The presented methodology is applicable to clay mineral characterization for various chemical and mineralogical investigations, for geochronological dating and regional tectonic studies.

2. CLAY-SIZE SEPARATION: Material and Methods

2.1. Sample descriptions

Fifteen samples were used for clay-mineral separation. Ten samples are clay-rich fault gouge and consist of friable portions of host rocks affected by fault activity. Fault gouges were collected along the trace of subvertical faults (e.g., Fig. 1a) and originate from various lithologies (Fig. 1b). Five samples are variably altered basement rocks with a pelitic protolith which have altered to different types of clay minerals (Table 1, Fig. 1c). Each of the fifteen samples comprised about 1-1.5 kg of crumbly material, including larger pieces, chips, and silt/clay-rich portions (Fig. 1b, c).

Figure 1. (a) Example of outcrop from which one of the samples was collected. In the photo, the red arrow points to a fault zone belonging to the King Salmon Thrust, with the fault locally separating dark grey from white carbonates. (b) examples of fault gouge (from the fault in Fig. 1a) and of (c) an altered basement rock from Millennium Uranium Deposit.

Table 1. Sample location (WGS84, GPS coordinates) and main information.

Sample	Location	Elevation (m)	Reference location	Host rock type
22KNA003A001	59.8573425; 134.79179533	751.3	Llewellyn Fault	Fault gouge sample
22KNA004B01	59.869619; 134.78926183	733.1	Llewellyn Fault	Fault gouge sample
22KNA0012C01	59.95531983; 134.71362317	848.1	King Salmon Fault	Fault gouge sample
22KNA0027A01	58.700391; 133.634849	0.0	Llewellyn Fault	Fault gouge sample
22KNA0029A01	58.700159; 133.633424	0.0	Llewellyn Fault	Fault gouge sample
22PVA-19-CX-057-4	57.52109700; -105.63468600	536.8	Millennium Uranium Deposit	Altered pelitic (sampled the basement rock alteration)
22PVA-20-CX-057-4	57.52109700; -105.63468600	536.8	Millennium Uranium Deposit	Altered pelitic (sampled the basement rock alteration)
22PVA-21-CX-064-1	57.52267900; -105.63431300	534.4	Millennium Uranium Deposit	Altered pelitic (sampled the basement rock alteration)
22PVA-39-CX-094	57.51913200; -105.63590400	536.8	Millennium Uranium Deposit	Altered pelitic (sampled the basement rock alteration)
22PVA-40-CX-094	57.51913200; -105.63590400	536.8	Millennium Uranium Deposit	Altered pelitic (sampled the basement rock alteration)
23KNA-LN0004 B01	59.81267383; -134.71913683	1622	Llewellyn Fault	Fault gouge sample
23KNA-LN0004 B02	59.81267383; -134.71913683	1622	Llewellyn Fault	Fault gouge sample
23KNA-LN0004 B03	59.81267383; -134.71913683	1622	Llewellyn Fault	Fault gouge sample
22LAV-003 122.46-123.00	59.22161791; -134.11887578	721	Llewellyn Fault	Fault gouge sample
22LAV-003 123.54-124.00	59.22161791; -134.11887578	721	Llewellyn Fault	Fault gouge sample

2.2. Sample preparation: freeze-thaw and freeze-drying.

Fault gouge and altered basement rocks often manifest as crumbling materials wherein clay materials are agglutinated on, or adhered to, cobbles, gravels, and finer earth material. Traditional rock crushing equipment or hand-crushing techniques using a mortar and pestle to disaggregate the finer from the coarser grain size fractions can lead to artificial grain size reductions for coarse relicts of K-bearing minerals. This can affect the mineralogy and crystallinity of the clay size fractions (Kisch, 1991). To mitigate the alteration of parent material and accurately trace grain size-dependent age variations in individual clay fractions, a careful sample disaggregation method is recommended (Liewig et al., 1987). This involves subjecting the samples to repetitive freeze-thaw cycles (Liewig et al., 1987; Zwingmann and Mancktelow, 2004; Torgersen et al., 2015a, b) to induce clast breakage, facilitated by the increase in water volume within intercrystalline fractures and grain boundaries.

In this protocol, the samples are transferred into 1 L wide-mouth HDPE bottles and submerged with distilled water. They undergo cycles of deep-freezing at temperatures of -50±1 °C for a minimum interval of approximately 1 to 1.5 hours (i.e., until the distilled water within each

container is frozen), followed by thawing in a warm water bath set at around 30±2 °C (87-90 °F) for approximately 45-60 minutes. The number of freeze-thaw cycles required to disaggregate a sample is dependent on lithology and environmental parameters (Othman et al., 1994), but in general ~90 cycles of freeze-thaw on granitic gouges can be reduced to ca. 15-20 cycles for more friable altered samples. To expedite the disaggregation process and reduce the number of freeze-thaw cycles in hard competent blocks, an initial mechanical crushing can be employed to induce fracture propagation, thereby enhancing hydraulic conductivity and water penetration during subsequent freeze-thaw events.

After the cycles of freezing and thawing, the distilled water is removed from the samples by freeze-drying. First, samples are transferred to a freezer set at -50°C until freezing process is complete. Then, containers are transferred (without lids but covered by a small square of low-linting precision paper wiper fixed with elastic bands) into a Labconco FreeZone 12L Freeze Dryer. The collector chamber operates at -48/-50 °C and collects the water vapor extracted from the sample while exposed to vacuum conditions (< 0.2 mbar; typically, ~ 0.08 mbar).

2.3. Clay-size separation

2.3.1. Sieving

Freeze-drying can result in minor clay agglutination because, without inter-crystalline water, they attract and adhere to each other due to their charged surfaces. When this happens, samples can be gently disaggregated with a mortar and pestle by a single delicate tap. Freeze-dried samples are split to obtain an amount of between 400 and 800 g of material, while part of the original sample is archived for future investigations (Table 2). To produce equal subsamples, splitting is performed by means of a stainless-steel Jones Riffle Splitter (Fig. 2a) consisting of twelve opposing inclined chutes (width of 2 cm). These steps are repeated until the required amount of sample is obtained (Girard et al., 2004).

Subsamples are then transferred into a stainless-steel solderless sieve stack with mesh sizes of 2 mm, 250 µm, and 63 µm. Mechanical (dry) sieving is performed with the aid of a Retsch AS-400 sieve shaker, inducing 15 second vibration intervals with an amplitude of 2.1 mm for 10 minutes (Fig. 2b, Table 2). Of the fractions collected (Fig. 2c), the >250 µm is weighed and set aside, the less then 63 µm is weighed and transferred into the 1000 mL centrifuge bottle, and the 63-250 µm fraction is set aside for wet sieving to recover the <63 µm grains stacked between the

coarser grains (Fig. 2d). For wet sieving, a slurry of the 250-63 µm fraction is made with about 250 mL of distilled water by mixing them together in a stainless-steel bucket with a milkshaker mixer. The slurry is transfer into a 63 µm sieve setup on top of a 1000 mL centrifuge bottle already containing the <63 µm sieve fraction. Wet sieving is accelerated by gently moving the heterogeneous mixture with (gloved) fingers over the sieve, washing with distilled water allowing finer material to migrate through the mesh until a total weight of 750-800 g (sample and distilled water) is collected (Fig. 2d).

Table 2. Sieving parameters and results. In column two, "Starting weight (g)" indicates the sample weight after splitting. In column three and four, the weights are those measured after dry sieving but before wet sieving. The stored fraction is that of the sample subjected to sieving and does not account for the archived split portion.

sample	starting weight (g)	<63 µm fraction weight (g)	63-250 µm fraction weight (g)	stored >250 µm fraction (g)
22KNA0029A01	599.8	74.3	108.9	416.5
22KNA0012C01	387.5	22.4	105.4	250.7
22KNA0027A01	447.9	29.7	61.1	345.8
22KNA003A001	399.6	22.1	51.5	323.7
22KNA004B01	566.2	12.7	55.4	498.2
22PVA-19-CX-057-4	215.1	1.9	40.1	173.1
22PVA-20-CX-057-4	388.2	10.1	18.4	359.7
22PVA-21-CX-064-1	429.6	5.1	12.5	412.1
22PVA-39-CX-094	425.4	5.4	17.0	403.0
22PVA-40-CX-094	252.2	5.0	9.7	237.6
23KNA-LN0004 B01	1528.8	56.6	197.1	1295.4
23KNA-LN0004 B02	846.4	28.1	117.3	689.5
23KNA-LN0004 B03	682.2	26.1	98.9	549.1
22LAV-003 122.46-123.00	695.4	17.7	46.3	620.8
22LAV-003 123.54-124.00	588.0	8.8	22.8	551.2

Figure 2. (a) Jones riffle splitter device. (b). Mechanical (dry) sieving was performed with the aid of a sieve shaker. (c) Different grain size fractions after dry sieving (from top right to bottom left: >2 mm; 250 µm-2 mm; 250-63 µm; <63 µm fraction). (d) wet sieving of the heterogeneous mixture of the 63-250 µm fraction and distilled water.

2.3.2. Centrifugation

Centrifugation is a widely used technique for separating particles of different sizes (e.g., isolating specific silt and clay fractions) and densities from a suspension with a known (or estimated) size distribution of particles. At the Sedimentology Laboratory at the GSC (Ottawa), centrifugation is performed with two different centrifuges: a Sorvall Centrifuge (Model RC3C plus), for a maximum speed of about 2200 RPM, and an International Centrifuge (IEC) (Model UV PR-7000), at a speed up to 3500 RPM. Both achieve grain size separation through conventional centrifuge rotors in which swinging buckets holding sample tubes (Nalgene centrifuge bottles with a capacity of 1000 mL) are spun around a central axis at high speeds, causing the buckets to swing outwards and orient the samples perpendicular to the axis of rotation. As the rotor spins, the centrifugal force causes coarser particles in the samples to separate based on their density. Ideally, denser particles move outward more quickly and pellet to the bottom of the centrifuge bottle, while less dense particles remain suspended as supernatant (Fig. 3).

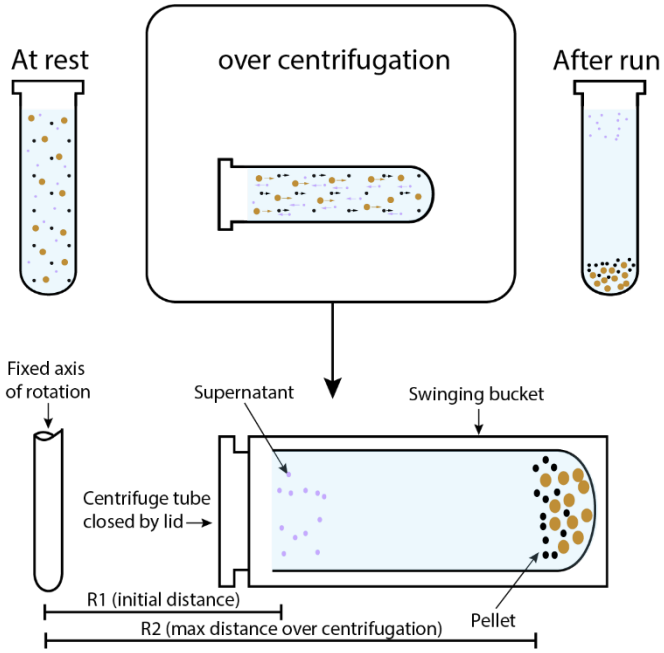

Figure 3. Sample orientation in swinging-bucket. Purple particles dispersed in distilled water are separated by density from black and orange denser/coarser particles. Please note that finer/less dense fractions can be trapped by coarser particles (or grains) during centrifugation (modified after Poppe et al., 2001).

The time (t) to settle the pellet at the bottom of the bottle is estimated by means of Stokes' law, as:

$$(1)\quad t = \frac{9\eta \ln\left(\frac{R2}{R1}\right)}{8\pi^2 N^2 r^2 (\rho - \rho_0)} + \frac{2(ta+td)}{3}$$

where t is the total time (in seconds), η is the viscosity, R1 is the initial distance from the axis of rotation when the bucket is in the vertical position (Fig. 3), R2 is the final distance from the axis of rotation when the bucket is in the horizontal position (Fig. 3), N is the angular velocity, r is the particle radius, ρ is the density of the particle, ρ_0 is the density of the displaced media (distilled water), *ta* is the time required for acceleration of the rotor, and *td* is the time of deceleration (Jackson, 1967). For the present protocol, R1 is about 16 cm and R2 is about 25 cm. Quartz is used as a reference material for the ρ density of the particle (2.65 g/cm³); the liquid density is estimated as 0.9997 g/cm³ at 20°C for ρ_0; and the water viscosity as 0.0102 g/(s·cm) at 20°C. Five speeds (set as *revolutions per minute*, RPM) were chosen for fractionating the different grain sizes (for speeds and time intervals, see Table 3).

The separation process starts with the slurry containing the <63 µm fraction (Fig. 4a-c) and proceeds to progressively finer fractions over subsequent steps for *ca*. 3 hours allowing to obtain the 63–10 µm, 10–6 µm, 6–2 µm, 2–0.6 µm, 0.6–0.2 µm, and <0.2 µm fractions. Six to seven wide-mouth plastic jars ranging from 0.1 to 1 L (chemical-resistant polypropylene, suitable for freeze-drying) are also weighed and labeled according to the expected silt/clay size corresponding to their hydrodynamic diameter. After centrifugation, the separated fractions are transferred into the wide-mouth plastic jars for freezing at -50°C and then freeze-drying to remove all the excess distilled water used for centrifugation (Fig. 4d-e). The detailed step-by-step protocol is provided in the Appendix (A.1 section).

Table 3. Centrifugation parameters and steps, as described in the text. Each bar corresponds to the number of centrifugation cycles at the corresponding RPM and time. "Decant" refers to the step where supernatant suspensions are separated from the sedimented material pellets and transferred to a new bottle. "Cleaning" indicates the step aimed at removing any coarse particles accidentally transferred in the bottle along with the supernatants after the "decant" step. "Wash" indicates a centrifugation step aimed at removing any unwanted finer material trapped between the pellets after "decant" and "cleaning". See section A.1 in the Appendix for further details.

Fraction	Fraction 1 *63-10 µm*	Fraction 2 *10-6 µm*	Fraction 3 *6-2 µm*	Fraction 4 *2-0.6 µm*	Fraction 5 *0-6-0.2 µm*	Fraction 6 *<0.2 µm*
Decant	|	|	| |	||	| |	-
Cleaning	|	|	| |	||		-
Wash	|	|	|	||		-
RPM	150	250	750	2200	3500	-
Time (mins)	3:45	3:54	4:14	6:00	18:00	-

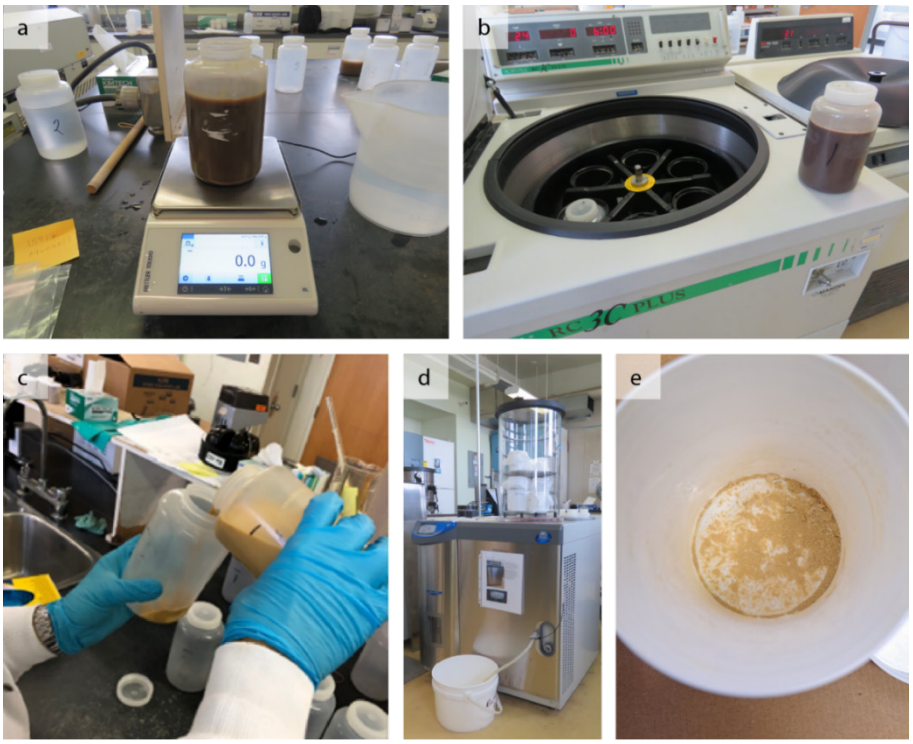

Figure 4. (a) Example of Bottle #1 filled with the slurry containing <63µm fraction; balance used to weigh samples for placing in centrifuge (b) Sorvall Centrifuge. (c) Decanting of fine-grained supernatant from Bottle #1 into Bottle #2, ensuring avoidance of re-suspension of pelleted material at the bottom of the Bottle #1. (d) Labconco FreeZone 12L Freeze Dryer console and sample chamber. (e) example of <2 µm material collected in a jar after centrifugation and freeze-drying.

To test the protocol, the grain size of the separated samples was checked by means of a Beckman Coulter 13320 laser particle size analyzer (e.g., Fig. 5). A quantity of about 0.2-0.1 g was transferred into a small beaker along with an aqueous solution of sodium hexametaphosphate (50g/L) to disperse the clay particulates. Prior to particle size analysis, samples were sonicated for 2 minutes to maximise the separation of particles.

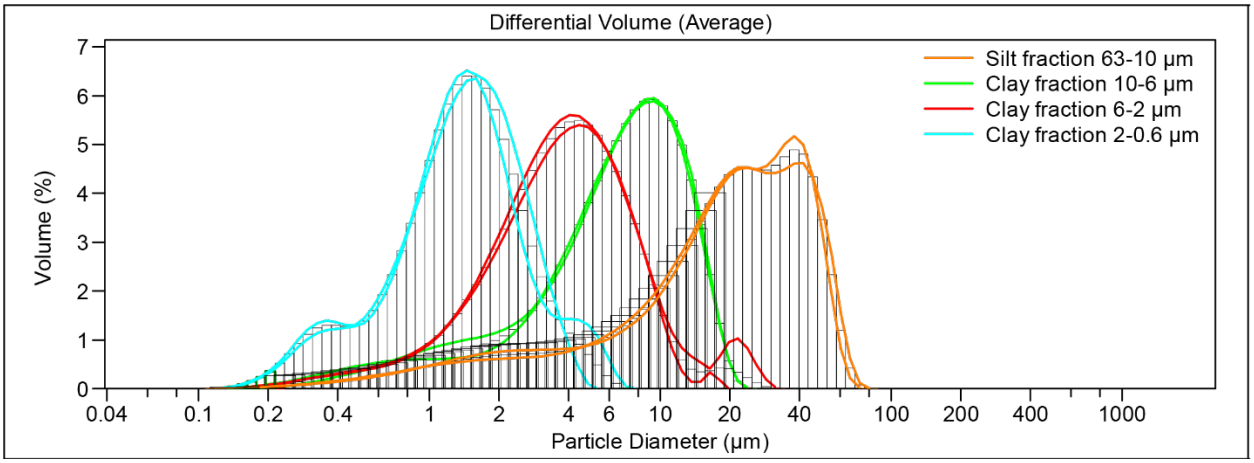

Figure 5. Representative grain size distribution plots of some of the fractions extracted from one sample.

3. X-RAY POWDER DIFFRACTION ANALYSIS

3.1. Sample preparation and X-ray Diffraction analysis

X-ray diffraction (XRD) analysis is conducted on the various grain size fractions to investigate the relationship between protolith mineralogy and the geological conditions resulting in clay authigenesis (e.g., McIntosh et al., 2021). For this purpose, the X-ray Mineralogy Laboratory at the GSC (Ottawa) is equipped with a Bruker D8 Advance X-ray powder diffractometer with a Lynxeye detector, Co Kα X-ray tube operating at 35 kV and 40 mA.

For silt samples between 63 and 10 µm, a McCrone micronizing mill is used for pulverizing the material to about 5-10 µm grain size prior to XRD analysis (see A.2 section in the Appendix). For identification and quantitative mineralogy, 3-5 g of the pulverized material is back pressed into an Al holder to produce a randomly oriented sample for analyses. Finer clay-fractions (10-6 µm, 6-2 µm, 2-0.6 µm, 0.6-0.2 µm, <0.2 µm) are prepared as air-dried samples. A quantity of 40 mg of the material is suspended in about 1.5 mL of distilled water, mixed using a Vortex Mixer for about 1 minute and then pipetted onto glass slides to produce oriented samples. These mounts are air-dried overnight and then run on the XRD. A continuous scan with the Bruker D8 Advance X-ray powder diffractometer is performed over a range of 2 to 86° 2θ with a step scan of 0.024° for pressed powders and of 0.029° for clays (slit mode variable for pressed powders and fixed for clays).

Follow-up treatments include a 48-hour long vapour treatment to saturate with ethylene glycol (EG) and heat treatment at 550 °C for 2 hours (see A.2 section in the Appendix). The EG-treatment is intended to determine the presence of expandable clay minerals such as smectite and the presence of mixed-layer clay minerals. A continuous scan is performed over a range of 2° to 86° 2θ for EG-treated samples, whereas heat-treated smears are scanned from 2° to. 35° 2θ.

For data processing, a computer-based software EVA 6.104 (Bruker AXS, Inc.) is used for characterization (Fig. 6) with comparison to reference mineral patterns using Powder Diffraction Files (PDF, licensed database PDF-5+ 2024) of the International Centre for Diffraction Data (ICDD). The XRD patterns for air-dried, ethylene glycol saturated and heat-treated samples are compared together (Fig. 6) to verify X-ray peak changes including shifts, increased intensity and disappearance allowing identification of certain clay minerals.

3.2. Mineral quantitative analysis

Quantitative analysis is carried out on the silt (63-10 µm) randomly-oriented fraction using TOPAS v. 5 (Bruker AXS, Inc.), a PC-based program that performs Rietveld refinement of the XRD patterns. In the Rietveld (1969) refinement method, the observed diffraction spectrum of a crystalline sample is compared with a theoretical diffraction pattern of reference minerals. A whole pattern fitting algorithm involves adjusting the parameters to minimize the difference between the observed and calculated (.cif files, structure files) diffraction patterns.

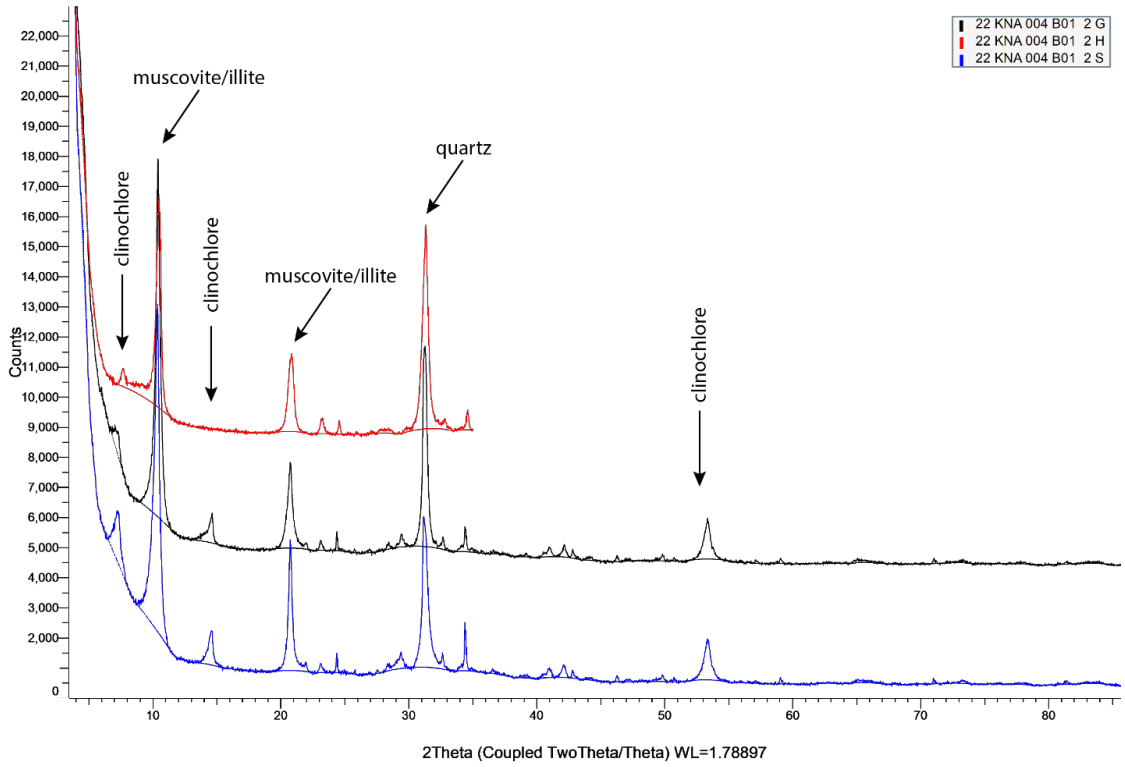

Figure 6. Stacked XRD pattern of a clay-size fraction (10-6 µm) after air-dried sample-preparation (22KNA004B01-2 S), ethylene glycol saturation (22KNA004B01-2 G), and heat treatment (22KNA004B01-2 H). No background removal nor smoothing applied. Y-offset added to highlight the different spectra. Note how the chlorite peak at 7 Å disappears after heat-treatment. Data are visualized through EVA 6.104 software.

The quality of the refinement (i.e., how well the calculated diffraction pattern matches the XRD data) is assessed by the Goodness of Fit (GoF) using a statistical approach that compares the observed and the calculated intensities for each peak position in the diffraction pattern for the standard deviation associated with the observed intensity at data point. A lower GoF value indicates a better agreement between the observed and calculated intensities. The main limitations for Rietveld refinement for quantitative analysis are that the .cif structure files for the calculated

diffraction patterns may be limited, so that an exact match to the mineral being analyzed may not be found. In turn, when expandable layers or mixed layer-clay minerals are encountered, or when mineral species have overlapping X-ray peaks (*e.g.*, chlorite and kaolinite), it can be more complicated to properly identify the minerals and quantify their abundance.

3.3. Mineral semi-quantitative analysis and crystallinity index

For the finer grained clay-size fractions, prepared as air-dried, EG-treated, and as heat-treated samples, Rietveld refinement is complicated by the preferred orientation that enhances the clay minerals (*00l*) peaks relative to the other *hkl* peaks. For this reason, only semi-quantitative analyses (Fig. 7) can be conducted using the Reference Intensity Ratio (RIR) method in EVA 6 software (Bruker AXS, Inc.).

The RIR method is based on the iterative comparisons between the relative intensities of the XRD diffraction peaks to those of an internal standard. By convention, corundum is selected as the standard as it has sharp and well-defined diffraction peaks over a wide range of diffraction angles. The RIR method utilizes the intensity ratio (I/Ic) of the mineral XRD spectra and the intensity of the corundum to normalize and scale all the X-ray peaks for each mineral phase to the standard. The assumption is that all the factors affecting the measured XRD pattern, except the abundance of the mineral in the aggregate, can be reduced to a constant, and therefore by using ratios and measuring peak areas, it is possible to estimate mineral abundances. Specifically, the I/Ic is calculated by taking the ratio of the strongest peak of the pattern to the intensity of the strongest peak of corundum in a 50/50 weight mixture. I/Ic ratios are experimentally determined and included in the PDF files (ICDD) of each reference mineral.

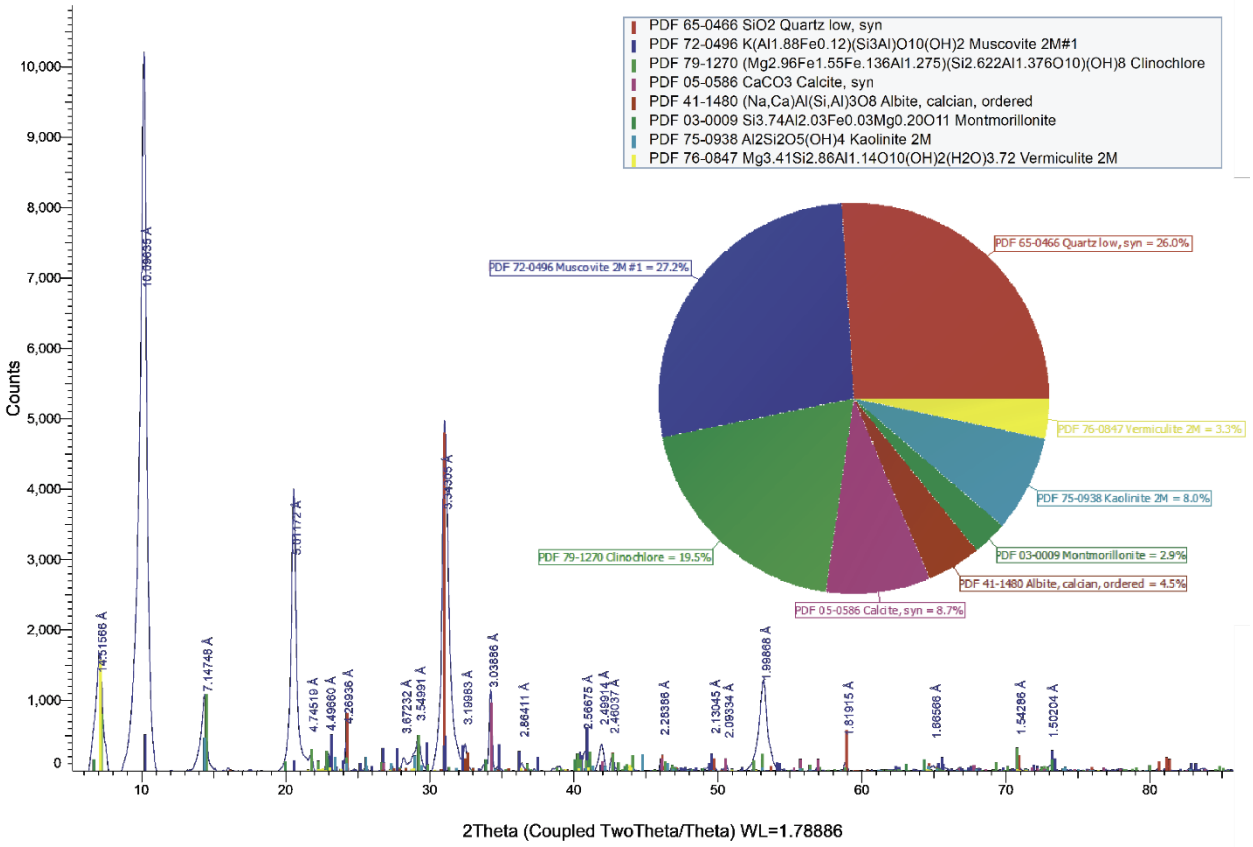

Figure 7. Example of semi-quantitative phase abundance estimation based on the mineral peak intensity.

The software EVA also allows for estimations of the minerals' crystallinity, for example, muscovite/illite (at 10 Å at (*001)* reflection) and chlorite (at 7 Å at (*002)* reflection plane), and of the crystallinity of the whole aggregate. The crystallinity of muscovite/illite (Kübler index) and of minerals from the chlorite group (Árkai index), measured in X-ray diffraction pattens as full-width-at-half-maximum (FWHM), are used to extrapolate the metamorphic conditions (and corresponding temperature regimes) under which the clay minerals developed, ranging from diagenetic to epizonal (Árkai, 1991; Kübler, 1967). However, the reproducibility of an estimate obtained with crystallinity methods significantly depends on sample preparation methods and diffractometer settings. For this reason, it is common practice to calibrate the crystallinity results of illite and chlorite obtained using standards. The GSC X-ray laboratory uses SW Crystallinity Index Standards (CIS) provided by the Swiss National Museum in Bern (Warr, Pers. Comm., 2020).

After conducting an XRD analysis on the standards and comparing the crystallinity values provided for the CIS standards with those measured at the GSC laboratory (Table 4), a calibration curve is calculated (Fig. 8) so that the crystallinity values can be extrapolated from unknown samples.

Table 4. Kübler index values and Árkai index estimated as FWHM for air-dried standards (currently available CIS standards, see Warr, 2018) compared with FWHM estimates on the same air-dried standards at the Geological Survey of Canada, Ottawa, point-peak (calibration performed on March 11th, 2024).

	Illite		Chlorite	
	Warr (2018) CIS values	*GSC's Lab. FWHM values*	*Warr (2018) CIS values*	*GSC's Lab. FWHM values*
Sw1 1992	0.630	0.427		
SW1 2012	0.653	0.403		
SW2 2012	0.455	0.288		
SW3 2000	0.497	0.283		
SW3 2012	0.372	0.196	0.302	0.152
SW4 2012	0.361	0.236	0.316	0.204
SW5 2000	0.344	0.228	0.271	0.151
SW6 2012	0.267	0.168	0.264	0.151
SW7 2012	0.277	0.161	0.268	0.154

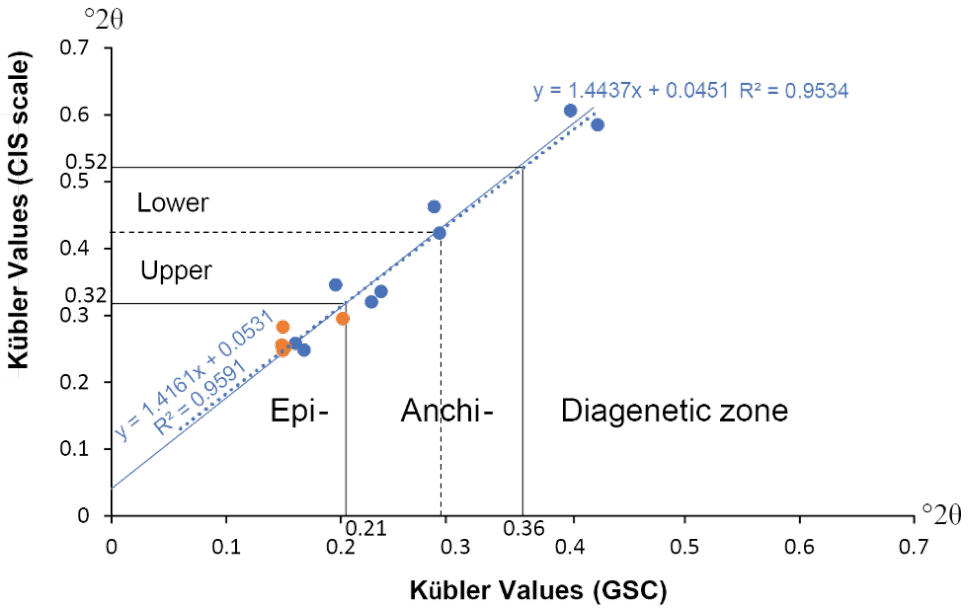

Figure 8. The FWHM correlation plot of the Kübler Index using the experimental CIS scale values and the laboratory values determined at the Geological Survey of Canada (see Table 4). The solid regression line represents the correlations for Kübler's index (9 points in blue), and the dashed regression line represents a correlation of both illite and chlorite values (fourteen points), which was used to calculate the CIS values for the new calibration. Kübler's anchizonal limits of 0.32°2θ and 0.52°2θ for the CIS scale, now translate to ca. 0.21°2θ and ca. 0.36°2θ for the current calibration at the GSC's laboratory.

4. DISCUSSION

The protocol presented here aims to recover a significant volume of fine-grained material from an original sample while avoiding the trapping of detrital grains from coarser fractions, grain breakage and amorphization of clay-size minerals. Among all the possible geological applications on separated clay size fractions (see the introduction section), this protocol particularly aligns with efforts to revive clay geochronology via $^{40}K–^{40}Ar$ at GSC laboratories. The $^{40}K–^{40}Ar$ technique was one of the earliest isotopic dating methodologies applied on rocks (Smits and Gentner, 1950) after the discovery of radioactive potassium (Aldrich and Nier, 1948), but it was progressively replaced by the $^{40}Ar/^{39}Ar$ dating technique (Merrihue and Turner, 1966) in which a portion of the ^{40}K is converted to ^{39}Ar via neutron irradiation. The $^{40}Ar/^{39}Ar$ method was considered a substantial improvement as dating only required mass spectrometry of Ar isotopes which results in greater internal precision and allows for an age to be measured on a single mineral grain instead of separate aliquots for K and Ar (Kelley, 2002). However, sample irradiation can cause recoil of the reactor-produced ^{39}Ar, which in fine-grained minerals such as illite and clay-size micas, can cause a conspicuous Ar loss from the crystal lattice and an increase in $^{40}Ar/^{39}Ar$ date (Clauer et al., 2012; Clauer, 2013). For this reason, the $^{40}K–^{40}Ar$ technique has been "re-discovered" and increasingly applied over the last decade for precise age determination of fault zone and hydrothermal deposits (e.g., Zwingmann and Mancktelow, 2004; Mottram et al., 2020) and aligns with the scientific priorities of the GSC's GeoMapping for Energy and Minerals (GEM-GeoNorth) and Targeted Geoscience Initiative (TGI-6) research programs. Effective application of this approach requires careful monitoring of grain size and mineral composition in datable minerals, as well as relatively large samples of at least 20-50 mg. Ensuring a good quantity of fine material is not simple and requires rigorously following the separation steps (*e.g.*, A.1 section in the Appendix).

Some of the procedures described here are manual (*i.e.*, freeze-thawing), thereby prolonging the time required to complete the protocol compared to if the same operations were automated. For example, many clay geochronology laboratories use a refrigerated/heated circulating bath with programmable timers. In these baths, samples bottles are submerged in a mixture of ethylene glycol and water which improves the effectiveness of the freeze-thaw cycles as the solution has a reduced freezing point compared to distilled water (see Othman et al., 1994), which reduces the time required to freeze and thaw the sample (about 1 hour).

We currently use conventional centrifuge rotors instead of flow centrifugation (also known as continuous flow centrifugation) to separate our finest grain sizes. Flow centrifugation allows for continuous introduction of large volumes of samples into the centrifuge rotor, at high centrifugal forces (good for separating down to nanometre-sized materials like nanoplastics and biological materials, *e.g.*, see Hildebrandt et al., 2020), reducing the time required for sample separation. However, swinging bucket rotors in conventional centrifuges are available at the GSC laboratories, are easy to use, and suitable for small quantities of material working at sufficient velocities for clay-size separation down to <0.2µm. We highlight that our estimates on time to sediment the coarse material (Table 4) are only applicable to swinging bucket centrifuges, where the pellet forms at the bottom of the centrifuge tube and were calibrated to the centrifuge model and bottles used at the GSC. These times must be modified for fixed angle rotor centrifuges (with pellet sedimentation on the side, which are usually faster but subjected to material losses caught in the angle of the tube; Jackson, 1967) and for flow centrifugation.

Aside from traditional centrifugation methods, many analytical laboratories have endeavored to implement or modify methods for the separation of clays into different grain size fractions for the $^{40}K–^{40}Ar$ geochronological technique (*e.g.*, Zheng et al., 2023). In this context, clay separation methods using "vacuum filtration" have been evaluated, proposed, and compared with classical centrifugation methods (Conn et al., 2016; Zheng et al., 2023). This method appears promising as it reduces the water used during centrifugation and improves the accuracy of the separated grain sizes by leveraging the intrinsic porosity of the membranes. In turn, this method may remove the need for further particle size analysis, for which a statistical amount of material would be needed (subtracting it from the already small quantities of clay material that it is often possible to separate for geochronological dating and chemical-mineralogical analyses). However, the main issue with this method is that, after repeated collection of the different clay-size fractions, the pores of the membranes can become obstructed. The pore size may decrease, resulting in the partial non-collection of material of the desired grain size. Additionally, this method does not account for the shape of clay minerals, as their acicular to flattened shape can affect their ability to pass through the pores at a given porosity. Ultimately, after XRD analysis, Zheng et al. (2023) demonstrated that centrifugation produces less infiltration of detrital minerals in the finer fractions than vacuum filtration. Therefore, our centrifuging procedure can be considered an effective

approach for producing different grain-size fractions for clay investigations, to be accompanied by mineralogical identification with XRD.

Regarding XRD analyses, the described method allows for obtaining not only qualitative but also quantitative and semi-quantitative information concerning the mineralogy of a polycrystalline aggregate for silt to clay-size aggregates. It also enables the determination of specific parameters, like the crystallinity index, valuable for geochronological and tectonic reconstructions/interpretations, as well as for analyzing the evolution of geological reservoirs for mineralization. A limitation of this protocol may lie in the clay-size sample preparation, for which air-dried oriented samples are used. Having samples with randomly oriented grains is the only way to ensure capturing all possible crystallographic planes and *hkl* peaks as clay minerals, owing to their platy, lathe, or fibrous morphology, would otherwise exhibit a preferred orientation, with the basal plane *(00l)* parallel to the sample holder. This affects the data processing for mineral quantification and for polytype characterization. Although preferred orientation correction can be applied during Rietveld refinement for quantitative analysis, as well as for the RIR method (section 3.3), specific peaks will be always enhanced for air-dried oriented mounts, while suppressing others. Also, masking some *hkl* peaks in the XRD pattern prevents discriminating the stacking sequences or crystallographic structures, specific for each polytype. However, a good polytype discrimination could be used to distinguish between igneous or metamorphic detrital micas from low temperature authigenic grains.

One effective method to obtain clay-bearing mounts with non-oriented grains for XRD involves the preparation of spherical aggregates via a Spray Dryer (Hillier, 1999). This process entails spraying the clay-size fraction in a solution (with polyvinyl alcohol) at low pressure (10-15 psi) into a dedicated oven, resulting in spherical droplets that are collected on a sheet of paper. This approach ensures that the clays within the droplets are not oriented. This apparatus, currently available at the GSC, could be implemented in the protocol when high-confidence quantitative estimations and polytype characterizations are required. In summary, the presented protocol for grain-size separation and XRD mineral characterization is tailored to common instrumentations like those at the GSC (Ottawa), but the underlying principles governing these procedures offer insights applicable to a wider analytical context.

REFERENCES

Aden, A. A., Wolfe, S. A., Percival, J. B., Grenier, A. (2015). Characteristics of glacial Lake McConnell clay, Great Slave Lowland, Northwest Territories. Natural Resources Canada. https://doi.org/10.4095/296860.

Aldrich, L.T., Nier, A.O. (1948). Argon 40 in potassium minerals. American Physical Society, 74 (8), 876. https://doi.org/10.1103/PhysRev.74.876.

Árkai, P. (1991). Chlorite crystallinity: an empirical approach and correlation with illite crystallinity, coal rank and mineral facies as exemplified by Palaeozoic and Mesozoic rocks of northeast Hungary. Journal of Metamorphic Geology, 9(6), 723-734.

Chamley, H. (1989). Clay Sedimentology. Springer-Verlag Berlin Heidelberg, Germany, 623 p. https://doi.org/10.1007/978-3-642-85916-8.

Clauer, N. (2013). The K-Ar and $^{40}Ar/^{39}Ar$ methods revisited for dating fine-grained K-bearing clay minerals. Chemical Geology, 354, 163-185. https://doi.org/10.1016/j.chemgeo.2013.05.030.

Clauer, N., Zwingmann, H., Liewig, N., Wendling, R. (2012). Comparative $^{40}Ar/^{39}Ar$ and K–Ar dating of illite-type clay minerals: a tentative explanation for the age identities and differences. Earth-Science Reviews. https://doi.org/10.1016/j.earscirev.2012.07.003.

Cloutier, J., Kyser, K., Olivo, G. R., Alexandre, P., Halaburda, J. (2009). The Millennium uranium deposit, Athabasca Basin, Saskatchewan, Canada: an atypical basement-hosted unconformity-related uranium deposit. Economic Geology, 104(6), 815-840. https://doi.org/10.2113/gsecongeo.104.6.815.

Conn, K.E., Dinicola, R.S., Black, R.W., Cox, S.E., Sheibley, R.W., Foreman, J.R., Senter, C.A., and Peterson, N.T. (2016). Continuous-flow centrifugation to collect suspended sediment for chemical analysis: U.S. Geological Survey Techniques and Methods, book 1, chap. D6, 31 p., plus appendixes, https://doi.org/10.3133/tm1D6.

Eberl, D.D., Drits, V.A., Środoń, J. (1998). Deducing growth mechanisms for minerals from the shapes of crystal size distributions. American Journal of Sciences 298, 499–533. https://doi.org/10.2475/ajs.298.6.499.

Fulignati, P. (2020). Clay minerals in hydrothermal systems. Minerals, 10(10), 919. https://doi.org/10.3390/min10100919.

Garven, G., Appold, M. S., Toptygina, V. I., Hazlett, T. J. (1999). Hydrogeologic modeling of the genesis of carbonate-hosted lead-zinc ores. Hydrogeology Journal, 7, 108-126. https://doi.org/10.1007/s100400050183.

Girard, I., Klassen, R. A. & Laframboise, R. R. (2004). Sedimentology Laboratory Manual, Terrain Sciences Division. Geological Survey of Canada, Open File, 4823. https://doi.org/10.4095/216141.

Hildebrandt, L., Mitrano, D. M., Zimmermann, T., Pröfrock, D. (2020). A nanoplastic sampling and enrichment approach by continuous flow centrifugation. Frontiers in Environmental Science, 8, 89. https://doi.org/10.3389/fenvs.2020.00089.

Hillier, S. (1999). Use of an air brush to spray dry samples for X-ray powder diffraction. Clay Minerals, 34(1), 127-135. https://doi.org/10.1180/000985599545984.

Hower, J., Hurley, P. M., Pinson, W. H., Fairbairn, H. W. (1963). The dependence of K-Ar age on the mineralogy of various particle size ranges in a shale. Geochimica et Cosmochimica Acta, 27(5), 405-410. https://doi.org/10.1016/0016-7037(63)90080-2.

Jackson, R. (1967). The Dynamics of Fluidized Particles. Cambridge: Cambridge University Press.

Kelley, S. (2002). K-Ar and Ar-Ar dating. Reviews in Mineralogy and Geochemistry, 47(1), 785-818. https://doi.org/10.2138/rmg.2002.47.17.

Kisch, H. J. (1991). Illite crystallinity: recommendations on sample preparation, X-ray diffraction settings, and interlaboratory samples. Journal of Metamorphic Geology, 9(6), 665-670. https://doi.org/10.1111/j.1525-1314.1991.tb00556.x.

Kübler, B. (1967). La cristallinité de l`illite et les zones tout à fait superieures du métamorphisme. In: Étages Tectoniques, Colloque de Neuchâtel 1966 (pp. 105-121), a La Baconniere, Neuchâtel.

Liewig, N., Clauer, N., Sommer, F. (1987). Rb-Sr and K–Ar dating of clay diagenesis in Jurassic sandstone reservoirs. American Association of Petroleum Geologists Bulletin, 71, 1467–1474. https://doi.org/10.1306/703C80EC-1707-11D7-8645000102C1865D.

McIntosh, J. A., Tabor, N. J., Rosenau, N. A. (2021). Mixed-layer illite-smectite in Pennsylvanian-aged paleosols: Assessing sources of illitization in the Illinois Basin. Minerals, 11(2), 108. https://doi.org/10.3390/min11020108.

Merrihue, C., Turner, G. (1966). Potassium-argon dating by activation with fast neutrons. Journal of Geophysical Research, 71(11), 2852-2857. https://doi.org/10.1029/JZ071i011p02852.

Mottram, C. M., Kellett, D. A., Barresi, T., Zwingmann, H., Friend, M., Todd, A., Percival, J. B. (2020). Syncing fault rock clocks: Direct comparison of U-Pb carbonate and K-Ar illite fault dating methods. Geology, 48(12), 1179-1183. https://doi.org/10.1130/G47778.1.

Ootes, L., Castonguay, S., Friedman, R., Devine, F., Simmonds, R. (2018). Testing the relationship between the Llewellyn fault, Tally-Ho shear zone, and gold mineralization in

northwest British Columbia. Geological Fieldwork, 2018-1. https://ostrnrcan-dostrncan.canada.ca/handle/1845/145141.

Othman, M. A., Benson, C. H., Chamberlain, E. J., Zimmie, T. F. (1994). Laboratory testing to evaluate changes in hydraulic conductivity of compacted clays caused by freeze-thaw: State-of-the-art. ASTM Special Technical Publication, 1142, 227-227. https://doi.org/10.1520/STP23890S.

Pevear, D.R. (1999). Illite and hydrocarbon exploration. Proceedings of the National Academy of Sciences of the United States of America, v. 96, p. 3440–3446. https://doi.org/10.1073/pnas.96.7.3440.

Poppe, L.J., Paskevich, V.F., Hathaway, J.C., Blackwood, D.S. (2001). Separation of the silt and clay fractions for X-ray powder diffraction by centrifugation, In: A laboratory manual for X-ray powder diffraction. Open-File Report 2001-41. https://doi.org/10.3133/ofr0141.

Richard, A., Cathelineau, M., Boiron, M. C., Mercadier, J., Banks, D. A., Cuney, M. (2016). Metal-rich fluid inclusions provide new insights into unconformity-related U deposits (Athabasca Basin and basement, Canada). Mineralium Deposita, 51, 249-270. https://doi.org/10.1007/s00126-015-0601-4.

Rietveld, H. M. (1969). A profile refinement method for nuclear and magnetic structures. Journal of Aapplied Crystallography, 2(2), 65-71. https://doi.org/10.1107/S0021889869006558.

Smits F, Gentner W (1950). Argonbestimmungen an Kalium-Mineralien I. Bestimmungen an tertiären Kalisalzen. Geochimica et Cosmochimica Acta 1:22-27. https://doi.org/10.1016/0016-7037(50)90005-6.

Tartaglia, G., Viola, G., van der Lelij, R., Scheiber, T., Ceccato, A., Schönenberger, J. (2020). "Brittle structural facies" analysis: A diagnostic method to unravel and date multiple slip events of long-lived faults. Earth and Planetary Science Letters, 545, 116420. https://doi.org/10.1016/j.epsl.2020.116420.

Torgersen, E., Viola, G. (2014). Structural and temporal evolution of a reactivated brittle–ductile fault – Part I: fault architecture, strain localization mechanisms and deformation history. Earth and Planetary Science Letters, 407, 205–220. http://dx.doi.org/10.1016/j.epsl.2014.09.019.

Torgersen, E., Viola, G., Zwingmann, H., Harris, C. (2015a). Structural and temporal evolution of a reactivated brittle–ductile fault–Part II: Timing of fault initiation and reactivation by K–Ar dating of synkinematic illite/muscovite. Earth and Planetary Science Letters, 410, 212-224. http://dx.doi.org/10.1016/j.epsl.2014.09.031.

Torgersen, E., Viola, G., Zwingmann, H., Henderson, I. H. (2015b). Inclined K–Ar illite age spectra in brittle fault gouges: effects of fault reactivation and wall-rock contamination. Terra Nova, 27(2), 106-113. https://doi.org/10.1111/ter.12136.

Velde, B. (1985). Clay Minerals: A Physico-Chemical Explanation of their Occurrence. Wiley-Blackwell. https://doi.org/10.1007/978-3-662-12648-6.

van der Pluijm, B. A., Hall, C. M., Vrolijk, P. J., Pevear, D. R., Covey, M. C. (2001). The dating of shallow faults in the Earth's crust. Nature, 412(6843), 172-175. https://doi.org/10.1038/35084053.

Viola, G., Scheiber, T., Fredin, O., Zwingmann, H., Margreth, A., Knies, J. (2016). De-convoluting complex structural histories archived in brittle fault zones. Nature Communication 7, 13448. https://doi.org/10.1038/ncomms13448.

Viola, G., Torgersen, E., Mazzarini, F., Musumeci, G., van der Lelij, R., Schönenberger, J., Garofalo, P.S. (2018). New constraints on the evolution of the Inner Northern Apennines by K-Ar dating of late Miocene-Early Pliocene Compression on the Island of Elba, Italy. Tectonics. https://doi.org/10.1029/2018tc005182.

Warr, L.N. (2018). A new collection of clay mineral 'Crystallinity'Index standards and revised guidelines for the calibration of Kübler and Árkai indices. Clay Minerals, 53(3), 339-350. https://doi.org/10.1180/clm.2018.42.

Warr, L.N., Cox, S. C. (2016). Correlating illite (Kübler) and chlorite (Árkai) "crystallinity" indices with metamorphic mineral zones of the South Island, New Zealand. Applied Clay Science, 134, 164-174. https://doi.org/10.1016/j.clay.2016.06.024.

Warr, L.N., Mählmann, R. F. (2015). Recommendations for Kübler index standardization. Clay Minerals, 50(3), 283-286. https://doi.org/10.1180/claymin.2015.050.3.02.

Zheng, Y., Li, H., Li, J., Zhang, G., & Si, J. (2023). A comparison study of synkinematic illite isolation, quantitative X-ray powder diffraction, and K-Ar dating for direct fault gouge analyses. Acta Geologica Sinica-English Edition, 97(2), 636-650).

Zwingmann, H., Mancktelow, N. (2004). Timing of alpine fault gouges. Earth and Planetary Science Letters, 223(3-4), 415-425. https://doi.org/10.1016/j.epsl.2004.04.041.

Zwingmann, H., Yamada, K., & Tagami, T. (2010). Timing of brittle deformation within the Nojima fault zone, Japan. Chemical Geology, 275(3-4), 176-185.

APPENDIX A

A1. Centrifugation Steps

The silt/clay extraction sequence is done through two main cycles of centrifugation, starting with the Nalgene centrifuge bottle containing the <63 μm fraction (section 2.3.2). Each centrifugation stage, conducted according to specific times and speeds (see section 2.3.2, eq. 1, Table 3), is done to separate the supernatant (fine material suspended in distilled water) from the pellet (residue at the bottom of the bottle) as illustrated in Fig. 3.

Each centrifugation run is carried out for different purposes, specifically:

- "Decant", step aimed to collect the supernatant separated from the pellet. The material in suspension is transferred into a new bottle corresponding to a finer grain size fraction compared to the pellet accumulated at the bottom of the original bottle.
- "Cleaning", to remove any coarse particles accidentally transferred in the bottle along with the supernatants after the "decant" step.
- "Wash", to remove from the sediments (of the desired fraction) any unwanted finer material trapped between the pellet after "decant" and "cleaning".

Hereafter, the step-by-step procedure is reported.

<u>First cycle of centrifugation: (to collect the 0.6-0.2 μm and < 0.2 μm fractions)</u>

1. Label the Nalgene centrifuge bottle having the <63 μm fraction as Bottle#1 (corresponding to Fraction 1 in Table 3) and weigh it, adding as much distilled water to match the weight (within +/- 0.5 g of each other) of a reference Nalgene bottle to balance the rotor. Note that Bottle#1 should contain a proper amount of distilled water to match the column height used to estimate the centrifugation time for the terminal velocity of a sphere falling in a fluid following Stokes' Law. Start the first centrifugation at 750 RMP for 4 min and 14 s, placing Bottle#1 and the reference Nalgene bottle into opposite sides of the rotor of the Sorvall Centrifuge after vigorously shaking Bottle#1 to homogeneously resuspend the powders in the distilled water (action necessary for each centrifugation cycle).

2. After centrifugation, carefully decant all the supernatant in the distilled water in a new Nalgene centrifuge bottle, avoiding resuspending the material deposited at the bottom of the bottle (hereafter called pellet). The transferred supernatant grain size should be <2 μm (Table 3), but grains of similar size can be still trapped in the pellet of Bottle#1. As the grain size of the material in the new bottle should correspond to Fraction 4 in Table 3, label the bottle as Bottle#4a and weigh it, adding as much as distilled water to match the weight of the reference bottle (within +/- 0.5 g of each other) to balance the rotor (always following the weight estimated parameters). For the next centrifugation cycle, use the same setting (750 RMP for 4 min and 14 s) to clean the residue in Bottle#4a from the coarser fractions accidentally transferred in it from Bottle#1. Transfer all the supernatant to a new Nalgene centrifuge bottle and the residual pellet back into Bottle#1 and dispose Bottle#4a in the sink for hand washing.

3. Label the new bottle as Bottle #4b, having an expected grain size of <2 μm, and add distilled water until matching the weight of the reference bottle. Centrifuge both bottles in the Sorvall Centrifuge at 2200 RPM for 6 min. After centrifugation, transfer the supernatant into a new Nalgene centrifuge bottle, avoiding resuspending the pellet. Label the new Nalgene centrifuge bottle as Bottle #5a, as the expected grain size of the transferred suspension is 0.6-0.2 μm (Fraction 5, see Table 3) and save the pellet inside Bottle #4b. The pellet expected grain size in Bottle #4b is now 2-0.6 μm.

4. Add distilled water to Bottle #5a until matching the weight of the reference bottle. Clean Bottle #5a by centrifuging it (along with the reference bottle) at 2200 RPM for 6 min in the Sorvall Centrifuge. Transfer the supernatant of Bottle #5a into a Bottle #5b, that should be now cleared of coarser particles accidentally dropped into Bottle #5a. Recombine the residual pellet of Bottle #5a with Bottle #4b.

5. Add distilled water to Bottle#5b and centrifuge it along with the reference bottle at 3500 RPM, for 18 min in the International Centrifuge (IEC) UV PR-7000. Transfer the supernatant (with expected grain size <0.2 μm) into a 1 L wide-mouth plastic jars (chemical-resistant polypropylene, suitable for freeze-drying), previously weighed empty (noting the weight of the empty container with lid in the logbook).

6. Label the jar and the lid with the sample identification number and the expected grain size fraction (<0.2 µm, Fraction 6, see Table 3) and cover the jar with a low linting precision wiper (secured by an elastic band). Place the jar in the freezer at -50°C. The jar should not be completely filled to avoid overflow during freezing.
   Keep aside Bottle #5b for a later cleaning at the end of the second cycle of centrifugation.

Second cycle of centrifugation: (to (re)collect all fractions, i.e., both previously uncollected and collected fractions)

7. The second cycle of centrifugation begins again with Bottle #1, containing primarily all the residue with a grain size between 63 and 2 µm, along with a few finer particles trapped among the coarser grains (in addition to the fine pellet transferred from the previous bottles during steps 2 and 4, i.e., Bottle #4a and Bottle #5a). After adding distilled water to match the weight of the reference bottle, and after vigorous shaking to resuspend the settled pellet, Bottle#1 is centrifuged in the Sorvall Centrifuge (along with the reference bottle) at 150 RPM for 3 min, 45 s (Table 3). This step aims to obtain a fraction <10 µm in suspension (Fraction 2). The suspension is transferred into a new bottle, labelled as Bottle #2a according to the expected grain size extracted.

8. As Bottle#1 can still have some minor traces of finer grains, and Bottle#2 can have some coarser residue from Bottle#1, both bottles are subjected to a further cycle of centrifugation at 150 RPM for 3 min and 45 s in the same centrifuge (Table 3) to separate the finer grains (<10 µm) from Bottle#1 and the coarser grains (>10 µm) from Bottle#2a. For this step, the two bottles are filled with distilled water to match the estimated weight and shaken to resuspend the pellet. There is no need to use the reference bottle to compensate the weight in the rotor, as Bottle#1 and Bottle#2a are already compensating each other. After centrifugation, the supernatant in Bottle#1 is discarded, while the suspension of Bottle#2a is transferred into a new bottle, labelled as Bottle #2b and having only grains with a size <10 µm. If the residual pellet in Bottle#2a is significantly high, it is then transferred into Bottle#1 for a further washing of Bottle#1 at 150 RPM for 3 min and 45 s. Otherwise (and more commonly), this pellet in Bottle#2a can be discarded.

9. The residual pellet in Bottle#1 is collected in a *ca*. 100 (to 200) mL wide-mouth plastic jar previously weighed with cap and labelled with the sample identification number and the expected grain size fraction (63-10 µm). The jar is then covered with a low linting precision wiper (secured by an elastic band) and placed in the freezer at -50°C.

10. Bottle#2b is decanted after centrifuging at 250 RPM for 3 min and 54 s ' in the Sorvall Centrifuge along with the reference bottle. The supernatant, with an expected grain size <6 µm (Fraction 3), is transferred as much as possible into a new bottle, labelled as Bottle#3a.

11. As Bottle#2b can still have some minor traces of finer grains, and Bottle#3a can have some coarser pellet from Bottle#2b, both are subjected to a further cycle of centrifugation at 250 RPM for 3 min and 54 s in the same centrifuge (Table 3) to wash Bottle#2b and clean Bottle#3a. For this step, the two bottles are filled with distilled water to match the estimated weight and shaken to resuspend the pellet. After this centrifugation, the supernatant in Bottle#2b is discarded in the sink, while the supernatant of Bottle#3a is transferred into a new bottle, labelled as Bottle #3b and having only grains with a size <6 µm with no contamination from coarser material (Fraction 3). If the residual part in Bottle#3a is significantly high, it is then transferred into Bottle#2b for a further washing of Bottle#2b at 250 RPM for 3':54". Otherwise (and more commonly), this residual pellet can be discarded.

12. The pellet settled at the bottom of Bottle#2b is collected in a 200 mL wide-mouth plastic jar previously weighed with cap and labelled with the sample identification number and the expected grain size fraction (10-6 µm, Fraction 2). The jar is then covered with a low linting precision wiper (secured by an elastic band) and placed in the freezer at -50°C.

The following steps mirror those performed for the first cycle of centrifugations, with the aim of collecting clay-size separates cleaned from any coarser (cleaning step) and finer fractions (washing step). The steps are detailed below.

13. Bottle#3b is centrifuged at 750 RPM for 4 min and 14 s' in the Sorvall Centrifuge along with the reference bottle, with which it shares the weight to balance the rotor of the

centrifuge. The supernatant, with an expected grain size <2 μm, is transferred as much as possible into a new bottle, labelled as Bottle#4b (corresponding to Fraction 4).

14. As Bottle#3b can still have some minor traces of finer grains, and Bottle#4b can have some coarser residue from Bottle#3b, both are subjected to a further cycle of centrifugation at 750 RPM for 4 min and 14 s in the same centrifuge (Table 3) to wash Bottle#3b and clean Bottle#4b. For this step, the two bottles are filled with distilled water to match the estimated weight and shaken to resuspend the pellet. After this centrifugation step, the supernatant in Bottle#3b is discarded, while the supernatant of Bottle#4b is transferred into a new bottle, labelled as Bottle #4c and having only grains with a size <2 μm with no contamination from coarser material (Fraction 4). If the residual part in Bottle#4b is significantly high, it is then transferred into Bottle#3b and a further washing of Bottle#3b is repeated at 750 RPM for 4 min and 14 s. Otherwise (and more commonly), this residue can be discarded.

15. The pellet settled at the bottom of Bottle#3b is collected in a 200 mL wide-mouth plastic jar previously weighed with cap and labelled with the sample identification number and the expected grain size fraction (6-2 μm). The jar without cap is covered with a low linting precision wiper (secured by an elastic band) and placed in the freezer at -50°C.

16. Bottle#4c is centrifuged at 2200 RPM for 6 min in the Sorvall Centrifuge along with the reference bottle. The supernatant, with an expected grain size <0.6 μm (Fraction 5, Table 3), is transferred as much as possible into a new bottle, labelled as Bottle#5c.

17. To prevent breakages or material losses, it is not necessary to repeat the centrifugation runs of the samples contained in the bottles Bottle#5c and Bottle#4c. The grain fractions have already been sufficiently cleaned during the previous centrifugation cycles and, most importantly, the concentration of crystals diluted in distilled water in the bottle is low, making it less likely for small grains to remain trapped with coarser grains at the bottom after decanting. Therefore, the pellet settled at the bottom of Bottle #4c is collected in a 500 mL wide-mouth plastic jar previously weighed with cap and labelled with the sample identification number and the expected grain size fraction (2-0.6 μm). The jar without cap

is covered with a low linting precision wiper (secured by an elastic band) and placed in the freezer at -50°C.

18. Bottle#5b, obtained during the 4th step of the first cycle of centrifugations, is now amalgamated with Bottle#5c and centrifuged at3500 RPM, 18 min cycle in the International Centrifuge (IEC) UV PR-7000. The supernatant in both bottles, with expected grain size <0.2 µm, is collected into a 1 L wide-mouth plastic jars (chemical-resistant polypropylene, suitable for freeze-drying), previously weighed empty. The jars without cap are covered with a low linting precision wiper (secured by an elastic band) and placed in the freezer at -50°C.

19. The decanted pellets in Bottle #5c and Bottle #5b are collected as fraction 0.6-0.2 µm (Fraction 5) in a 500 mL wide-mouth plastic jar previously weighed with cap and labelled with the sample identification number and the expected grain size fraction. The jars without cap are covered with a low linting precision wiper (secured by an elastic band) and placed in the freezer at -50°C.

20. At this point, all the clay-fractions have been extracted and stored in the freezer for at least 2 hours. Samples are then freeze-dried in a Labconco FreeZone 12L Freeze Dryer sample chamber to remove all the excess distilled water. The weight of each individual grain size fraction is obtained by re-weighing the respective wide-mouth plastic jar, closed with its original lid, and subtracting this new weight (accounting for the jar, lid, and dried sample) from the weight previously measured for the jar with the lid alone (Fig. 4d, e).

A2. XRD – Sample Preparation Steps

To produce pressed powders of the silt fractions (63-10 µm), the X-ray Mineralogy Laboratory at the GSC (Ottawa) is equipped with a micronizing mill (XRD-Mill McCrone by Retsch). This mill is specifically designed to preserve the crystalline structure during grinding (down to 5-10 µm) prior to X-ray diffraction analyses. Through the XRD-Mill McCrone the sample is pulverized by placing it, along with approximately 10 mL of isopropyl alcohol, in a

grinding jar with a 125 mL capacity, with 48 agate blocks (small cylindric blocks 1 cm in high and diameter, stacked using a loading device). The grinding jar is securely closed with a lid and fastened with a clamping bracket. After pulverizing, the jar is removed, and the cap is replaced with a pouring lid with two holes (smaller than the diameter of the agate blocks). The ground material is poured into a shallow weighing dish, using additional isopropyl alcohol to recover all the material, and is transferred to a fume hood to allow the alcohol to evaporate.

For finer clay-fractions (10-6 µm, 6-2 µm, 2-0.6 µm, 0.6-0.2 µm, <0.2 µm), 40 mg are suspended in 1.5 mL distilled water, thoroughly mixed using a Vortex Mixer and pipetted onto glass slides to air dry overnight. Following analyses the air-dried samples are placed in a desiccator containing ethylene glycol (EG), heated for about 20 minutes with a heat lamp to allow the vapours to circulate and penetrate the samples. The samples remain there for 48 hours and then are re-analysed.

After XRD analysis of the EG-treated clay-size fractions, samples are subjected to a heat treatment in a muffle furnace at 550°C for 2 hours (Fig. A1.e) and placed on the upper plate of a non-vacuum desiccator sitting above a base layer of granular desiccant (W.A. Hammond Drierite™ Drying Dessicants, Fig. A1. f) to avoid rehydration of minerals during cooling. When samples are cooled down (e.g., below 180°C), they are reanalyzed by XRD.

Figure A1. (a) Example of amount of fraction used to produce an oriented mount. (b) Samples suspended n distilled water and pipetted onto glass slides for air drying over night. (c) Oriented mounts in aluminium holders (numbers correspond to different clay-size fractions, as: (1) 10-6 µm, (2) 6-2 µm; (3) 2-0.6 µm, (4) 0.6-0.2 µm, and (5) <0.2 µm). (d) X-ray diffractometer with loaded aluminium holders with the clay-size mounts. (e) Desiccator jar used for EG-treatment. (f) Desiccator jar used after heat-treatment.